Generation of water-in-oil-in-water food emulsions enriched with magnesium by stirred cell membrane emulsification

Xiaolu Pu[1], Bettina Wolf[1*], Marijana Dragosavac[2]

[1]Division of Food Sciences, School of Biosciences, University of Nottingham,

Sutton Bonington Campus, Loughborough LE12 5RD, UK

[2]Chemical Engineering Department, Loughborough University,

Loughborough LE11 3TU, UK

[*]present address: School of Chemical Engineering, University of Birmingham, Birmingham B15 2TT

Highlights

- PGPR was used to stabilise internal water droplet interface
- Starch and pea protein isolate were used to stabilise w_1/o droplet interface
- Low energy membrane emulsification process generated stable $w_1/o/w_2$ emulsions
- Variation of shear stress and injection rate produced drops between 35 and 320 µm
- Complex food emulsifiers delayed release of Mg^{2+} ions for up to 2 weeks

Abstract

This study has for the first time shown that complex food emulsifiers such as starch and protein can be applied to produce stable w/o/w emulsions with the membrane emulsification technology. Using a microporous metal membrane with a 20 µm pore size, 2% of polyoxyethylene (20) sorbitan monolaurate (Tween 20), 4% of octenyl succinic anhydride (OSA) starch or 1.5% of pea protein isolate (PPI) in the external water phase respectively was the minimum concentration necessary to stabilise the w/o/w droplets. Uniform with a span as low as 0.45 and for at least 13-day stable w/o/w emulsions

of droplets between 35 and 320µm were obtained. The release of a magnesium tracer from the internal water phase of xanthan gum-thickened w/o/w emulsions, when OSA starch and PPI were used, was found to be limited to around 3% after 13-day storage. However, w/o/w emulsions stabilised with Tween 20 were less stable with magnesium showing a release of 27% on day 13.

Keywords: membrane emulsification; w/o/w emulsion; food; OSA starch; pea protein; delayed magnesium release.

1 Introduction

Water-in-oil-in-water (w/o/w) emulsions are aqueous emulsions where the included oil droplet phase contains small water droplets in a water-in-oil emulsion. Such emulsion microstructure offers the opportunity to entrap in a food systems materials for targeted release in the internal aqueous phase, for example, micronutrients such as metal supplements, flavours and vitamins during consumption (Herzi and Essafi, 2018, Manickam et al., 2018). The release profiles of those components will depend on the oils and surfactants used as well as the droplet size of the w/o/w emulsion (Leadi Cole and L. Whateley, 1997, Oppermann et al., 2018, Schuch et al., 2014, Schuch et al., 2013). Lower encapsulation efficiency of the inner water phase in w/o/w emulsions stabilised with polyglycerol polyricinoleate (PGPR) and egg yolk powder were found to correlate with smaller double emulsion droplet size independent of two emulsification methods (Schuch et al., 2014). On the contrary, Oppermann et al. (2018) showed that greater encapsulation efficiency of the inner water phase in w/o/w emulsions was correlated to smaller double emulsion droplet size. Tween 20, sodium caseinate and Whey protein isolate were used as stabilizers of the external water phase. Consequently, it is appropriate to seek a tool to control the droplet size of w/o/w emulsions independent of the hydrophilic emulsifier type and to investigate the impact of the hydrophilic emulsifier alone on encapsulation efficiency.

w/o/w emulsions are usually manufactured using a conventional two-step emulsification method based on high-pressure or high shear. However, these conventional methods rely on high energy input to disrupt the dispersed phase and form droplets (Schubert et al., 2003). The mechanical stress during processing tends to disrupt the emulsion droplets leading to a reduction in the encapsulation efficiency of the w/o/w emulsions (Kim et al., 2017). In contrast to this top-down processing approach, bottom-up processing technologies such as membrane emulsification and microchannel emulsification have been described in the literature as ways of obtaining a controllable droplet size while processing at much lower mechanical stress input (Schröder et al., 1998, Walstra and Smulders, 1998, Joscelyne and Tragardh, 2000, Schubert and Ax, 2003, Spyropoulos et al., 2014). Others often cited the advantages of bottom-up or mild emulsification processes to include increased energy efficiency as less energy is lost as frictional energy (Walstra, 1993, Joscelyne and Tragardh, 2000) and prevention of degradation or loss of functionality of heat and shear sensitive ingredients used to stabilise the emulsions, for example starch and protein (van der Graaf et al., 2005). In this research membrane emulsification, specifically stirred cell membrane emulsification (Kosvintsev et al., 2005, Dragosavac et al., 2008), was investigated as a process to generate similarly sized w/o/w emulsions of narrow droplet size distribution stabilised with different food emulsifiers.

PGPR, oil soluble surfactant, is commonly used in the oil phase of $w_1/o/w_2$ emulsions to stabilize the internal water phase (w_1) via top-down processing (Silva et al., 2018, Chen et al., 2018). The primary emulsion (w_1/o) is then applied to further top-down or alternatively bottom-up processing to create the final w/o/w emulsion where water soluble surfactant (most commonly Tween 20) must be present in the outer water phase (w_2). Another group recently reported on Tween 20 applied in the external aqueous emulsion phase to successfully stabilise w/o/w emulsions with encapsulated garlic extract via stirred cell membrane emulsification (Ilić et al., 2017, Nikolovski et al., 2018). Tween 20 is a small molecular weight surfactant with higher mobility compared to the macromolecules octenyl succinic anhydride starch (OSA) and pea protein isolate (PPI). OSA starch is native starch, often of the waxy type,

i.e., majorly consisting of amylopectin, that has been chemically modified to contain the anionic and nonpolar group – octenyl succinic anhydride. PPI mainly contains two globular proteins, legumin and vicilin (O' Kane et al., 2005). Globular proteins are rigid molecules and rearrange at the interface slowly (Stauffer, 1999). The starch and protein sorb slower at the droplet surface compared to Tween 20 but develop a thick and viscoelastic layer and stabilise the droplets through steric and electrostatic repulsion (Bhosale and Singhal, 2006, Dickinson, 2010). Therefore, comparison of drop stabilisation and encapsulation/release properties of starch, protein and Tween 20 would be beneficial.

However, to the best of our knowledge, there are no publications on the use of complex food emulsifiers such as starches and proteins to stabilise w/o/w emulsions via membrane emulsification. We were particularly interested in designing process conditions that would impart a comparable and narrow droplet size spectrum for both types of hydrophilic emulsifier, to then independently assess the release of magnesium encapsulated in the internal water phase. Magnesium was selected for convenient detection of release following previously published method (Bonnet et al., 2009). The emulsions, generated by stirred cell membrane emulsification, were thickened with the hydrophilic food hydrocolloid xanthan gum post emulsification to alleviate the impact of creaming on the results of the release measurement. Based on predictive modelling (Dragosavac et al., 2012), a formulation and processing protocol enabling the independent study of the impact of the choice of hydrophilic emulsifier on the release properties of a w/o/w emulsion, applicable to a broader choice of encapsulates than just magnesium, provided they will not alter the physico-chemical properties of the emulsion system, is introduced.

2 Materials and methods

2.1 Materials and emulsion phases

All used materials were food grade and were used without modifications. To match the osmotic pressure NaCl (Fisher Scientific, Loughborough, UK) was used both in the internal (w_1) and the external water phase (w_2) of $w_1/o/w_2$ emulsions. NaCl was selected as it enhances the adsorption of PGPR at the oil-water interface thus providing superior stability (Pawlik et al., 2010). NaCl, within the internal water phase (w_1), was replaced with $MgCl_2 \cdot 6H_2O$ (Sigma Aldrich, Dorset, UK) for easier and accurate detection of encapsulation efficiency or release. Internal water droplets (w_1) were stabilised in the oil phase (sunflower oil, purchased from local supermarket) with PGPR (PGPR 90; DuPont Danisco, Kettering, UK). Tween 20 (Sigma Aldrich, Dorset, UK), octenyl succinic anhydride (OSA) starch (N-creamer 46, Univar, Widnes, UK) and pea protein isolate (PPI) (MyProtein, Northwich, UK) were applied as a hydrophilic emulsifier. Xanthan gum (CP Kelco, San Diego, USA) was used as a thickening agent. Deionized (DI) water, produced on site, was used throughout this study, and sodium azide (Sigma Aldrich, Dorset, UK) was added to all aqueous phases to suppress microbial spoilage. Acetone (Sigma Aldrich, Dorset, UK) was used as a solvent for a membrane wetting agent (Micropore Technologies Ltd., Redcar, UK). All concentrations are provided on a weight by weight basis, unless stated otherwise.

The external water phases (w_2) were prepared by mixing the appropriate amount of hydrophilic emulsifier with 0.1M NaCl solution. For investigating the impact of emulsifier concentration on stirred cell membrane emulsification 0.5%, 1%, 2% and 4% Tween 20; 2% and 4% OSA starch; and 0.5%, 1.5%, 3% and 6% PPI were applied.

For encapsulation efficiency and release measurement, 1600 ppm Mg^{2+} ($MgCl_2 \cdot 6H_2O$, vacuum-dried overnight at 95°C to remove free moisture), was dissolved in water to constitute the internal aqueous phase (w_1) of the $w_1/o/w_2$ emulsions instead of 0.1 M NaCl. The outer water phase (w_2) consisted of 0.5% xanthan gum and 2% Tween 20, 4% OSA starch or 1.5% PPI. To maintain the osmotic pressure

119 balance between two aqueous phases of the w/o/w emulsions, Mg^{2+} concentration was calculated
120 according to Equation 1:

121 $$C_{Mg^{2+}} + 2C_{Cl^-} = C_{Na^+} + C_{Cl^-} = 2C_{NaCl} = 3C_{MgCl_2} = 0.2\ M \quad \text{Eq.1}$$

122 where $C_{Mg^{2+}}$, C_{Cl^-}, C_{Na^+}, C_{NaCl} and C_{MgCl_2} are molar concentrations of Mg^{2+}, Cl^-, Na^+ ions, NaCl and $MgCl_2$
123 present in w_1. It was checked that the addition of $MgCl_2$ to the w/o/w emulsions instead of NaCl had
124 no influence on the microstructure and droplet size distribution. The oil phase contained 4% PGPR and
125 was prepared by stirring for at least 30 min on a magnetic stirrer at room temperature.

126 The w_1/o emulsions, as the internal emulsion phase of the w/o/w emulsions, were produced by slow
127 addition of internal water phase (w_1) into the oil phase containing 4% PGPR under high shear mixing
128 (Ultra Turrax, model T25, IKA Works, Staufen, Germany) operating at 24000 rpm for 5 min.
129 Emulsification was performed in an ice bath to avoid overheating. These process conditions have
130 previously been reported to generate a droplet size of around 0.5 µm (Vladisavljevic and Schubert,
131 2003). Final concentration of internal water phase (w_1) within the oil phase was 40%.

132

133 2.2 Stirred cell membrane emulsification

134 For the preparation of the w_1/o/w_2 emulsions stirred cell membrane emulsification was used. A
135 hydrophilic nickel membrane with 4 cm diameter (Micropore Technologies Ltd., Redcar, UK),
136 containing uniform straight through 20 µm cylindrical pores with 200 µm pore spacing, was used (see
137 Figure A1 in the Appendix). Based on these two parameters, the porosity of the membrane
138 (Dragosavac et al., 2008) was calculated to be 0.91%. To increase the hydrophilicity of the membrane
139 and to avoid the spreading of the dispersed phase (w/o emulsions) over the membrane surface, the
140 membrane was pre-soaked for 30 min in 2% wetting agent (Micropore Technologies Ltd., Redcar, UK).

For a set-up the membrane was placed in the base of the Dispersion Cell (Micropore Technologies Ltd., Redcar, UK) filled with continuous phase.

After preparation of the base, a cylinder glass cell (125 cm^3 volume) was fitted over the membrane and filled with continuous phase (outer water phase (w_2)). A two-blade paddle stirrer, driven by a 24V DC motor and power supply (INSTEK Model PR 3060, UK), was fixed on the top of the cell. Maximum shear stress was controlled by rotational speed and ranged between 200 and 1500 rpm corresponding to a maximum shear stress at the membrane surface between 1 and 51 Pa depending on a continuous phase used. The dispersion phases (primary w_1/o emulsions) were injected through the microporous membrane surface using a syringe pump (AL-1000, World Precision Instrument, Hitchin, UK) fitted with a glass syringe of 29 mm inner diameter at constant injection rate in the range of 1 to 15 ml min^{-1} corresponding to a transmembrane flux between 70 and 1150 L h^{-1} m^{-2}. The experiments were continued until the dispersed phase volume fraction reached 10 or 30 vol.%. Once the desired amount of the w_1/o emulsion had passed through the membrane, the pump and the stirrer were switched off followed by transferring the w/o/w emulsion into a glass beaker (100 ml of w/o/w emulsion was prepared). Finally, 1 ml aqueous sodium azide solution was added to w/o/w emulsions to obtain a final sodium azide concentration of 0.02% to prevent microbial spoilage. The beaker was then covered with cling film and stored at room temperature (21 ± 5 °C) until further analysis.

After each use, the membrane was cleaned for 1 min with detergent solution in an ultrasonic bath followed by cleaning with acetone and DI water before drying using compressed air.

Injection speed and maximum shear stress applied to the membrane surface was varied depending whether the impact of formulation (type and concentration of hydrophilic emulsifier) or processing parameters on emulsion characteristics was evaluated. Emulsions were also produced to assess their microstructure stability and encapsulation or release properties. Parameter settings are evident from the presentation of the results.

165

166 2.3 Methods for acquisition of parameters required for the droplet diameter predictive model

167 To predict the droplet diameter (x) produced with the Dispersion Cell, a conventional shear force
168 model (Kosvintsev et al., 2005, Dragosavac et al. 2008) based on the balance between the capillary
169 force (function of equilibrium interfacial tension (γ) and pore size (r_p)) and the drag force (function of
170 a maximum shear stress (τ_{max}) and the droplet size (x)) acting on a strongly deformed droplet at a single
171 membrane pore was applied. The droplet diameter can be estimated according to Equation 2.

172 $$x = \frac{\sqrt{18\tau_{max}{}^2 r_p{}^2 + 2\sqrt{81\tau_{max}{}^4 r_p{}^4 + 4 r_p{}^2 \tau_{max}{}^2 \gamma^2}}}{3\tau_{max}} \quad \text{Eq.2}$$

173 Thus, to calculate the predicted droplet diameter, the interfacial tension between the w_1/o phase and
174 w_2 phases, the viscosity and the density of w_2 were measured as follows. All samples for these analyses
175 were prepared in triplicate and analysed once.

176 **Equilibrium interfacial tension** (γ) data at the interface between all the external aqueous emulsion
177 phases and the w_1/o emulsion was measured with a force tensiometer (DB2KS, White Electric
178 Instrument, Malvern, UK) using the Du Nouy ring method at room temperature (21 ± 5 °C). The
179 **viscosity** (20°C) of all the external aqueous emulsion phases was measured using a rotational
180 rheometer (MCR 301, Anton Paar, Graz, Austria) fitted with a concentric cylinder double gap geometry
181 (DG26.7/T200). Shear rate was stepped up at 5 points/decade between 0.1 and 1000 s^{-1} and a total
182 number of 21 points were acquired every 5 s. The **density** of external aqueous emulsion phases was
183 measured using a density meter (DMA 5000, Anton Paar, Graz, Austria).

184

185 2.4 Analysis of emulsion characteristics

186 The visual microstructure appearance and droplet size distribution of the produced emulsions were
187 analysed up to 13 days after processing (immediately after production; on day 1, 2, 6 and 13) to gain
188 insight into their microstructure stability.

189 The **microstructure** of the w/o/w emulsions was visualised using an epifluorescence microscope
190 (L3201LED, GT Vision Ltd., Suffolk, UK) operated in bright field illumination mode. Slides were
191 prepared by pipetting a few drops of the continuous phase (w_2) first, to reduce the influence of the
192 surface tension on drops, and then a few drops of emulsion onto a glass slide followed by carefully
193 sliding over a glass cover slip. At least three randomly selected areas of each slide were imaged at a
194 lower and a higher magnification (x4 and x20 objective) and three slides were prepared for each
195 emulsion.

196 The **droplet size distributions** were analysed with a laser diffraction particle size analyser (Malvern
197 Mastersizer 2000, Malvern Panalytical Ltd, Malvern, UK). The Dispersion cell was filled with deionized
198 water as the dispersing medium. Measurement set up and analysis was controlled by the instrument's
199 software package. The refractive index of the dispersion medium (water) and the dispersed phase (oil)
200 was set to 1.33 and 1.47, respectively. The absorption value of the dispersed phase was set to zero.
201 Once the emulsion was dispersed in the water, three measurements were taken, and the raw data
202 was fitted with a general model. Measurement was carried out in triplicate.

203

204 2.5 Preparation of xanthan gum thickened emulsions

205 To prevent creaming during encapsulation or release measurements, xanthan gum was added to the
206 emulsion after manufacturing. 1% xanthan gum solution was prepared by dispersing the xanthan gum
207 powder into water pre-heated to 80°C, while mixing at 1500 rpm with an overhead mixer (RW20 fitted
208 with a 4-bladed propeller stirrer, IKA, Staufen, Germany) for 1 h. The solution was left overnight to
209 cool down to room temperature (21 ± 5 °C) and to reach complete hydration before use. 70 g of

xanthan gum solution was added to 100 g of emulsion and mixed at 600 rpm on a magnetic stirrer for 30 min obtaining a final xanthan gum concentration in the external aqueous phase of the w/o/w emulsions of 0.5%. Using the particle sized analyser and microscope, it was confirmed that the droplet size and their distribution of the w/o/w emulsions did not change due to these mixing conditions.

2.6 Assessing magnesium (Mg^{2+}) encapsulation and release

An Atomic Absorption Spectrophotometer (Spectra AA-200 Varian, UK), operating at the wavelength of 285.2 nm, was used to detect Mg^{2+} concentration during the encapsulation and release study. Standard calibration curves with the Mg^{2+} concentration as a function of the measurement signal (absorbance) for different w_2 solutions are shown in Figure A2 in the Appendix. The absorption obtained from the spectroscopy increased with increasing magnesium concentration. The relationships were linear and repeatable.

To assess w_2 for leakage of w_1 and magnesium into w_2, the concentration of magnesium in w_2 was calculated based on the standard calibration curve. Magnesium release percentage was calculated as follows (Bonnet et al. 2009):

$$Mg\ (\%) = (C_{Mg} \cdot \varphi_{w_2}) / (C_t \cdot \varphi_{w_1})) * 100 \quad \text{Eq.3}$$

where C_{Mg} is the magnesium concentration in w_2, which was calculated from the corresponding calibration curves, made for each release media used. φ_{w_2} is the volume fraction of w_2 in final $w_1/o/w_2$ emulsion (0.8), φ_{w_1} is the volume fraction of w_1 in w_1/o emulsion (0.4) and C_t is the total Mg^{2+} concentration initially added in the internal water phase (1600 ppm). From the amount of Mg^{2+} released in the w_2 phase immediately after production (Figure 5; day 0) it is also possible to estimate

231 Magnesium encapsulation efficiency (*EE*) $EE\ (\%) = 100 - (C_{Mg}/C_t) \cdot (1 - \varphi_{w_2})/\ \varphi_{w_1} \cdot \varphi_{w_2}$ (Dragosavac et al.,
232 2012).

233 To prepare the samples for release analysis, a $w_1/o/w_2$ emulsion was centrifuged for 30 min at 3500
234 rpm (Heraeus Labofuge 400R, Thermo Scientific, Germany). The bottom layer was then carefully taken
235 out by pipette and centrifuged again at the same conditions to ensure that w_2 was void of oil droplets.
236 Via microscopic observation and droplet size analysis of the creamed emulsion droplets it was verified
237 that the chosen centrifugation conditions had not changed the droplet size distribution. All
238 measurements were taken over 13 days at the same days as emulsion droplet appearance was
239 checked.

240

241 # 3 Results and discussion

242 ## 3.1 Effect of emulsifier concentration

243 The effect of the surfactant concentration (Tween 20, OSA starch and PPI) and maximum shear stress
244 on the w/o/w emulsions droplet size and span have been jointly reported in Figure 1. Having in mind
245 that the model used to predict the droplet size using the Eq. 1 does not take into consideration the
246 injection rate, the experimental data are shown for the injection rate of 1 ml min^{-1} corresponding to
247 the lowest meaningful injection rate applicable in the experimental set-up. Increasing emulsifier
248 concentration led to a decrease in droplet size for the larger molecular weight emulsifiers PPI and OSA
249 starch, but not for Tween 20. At the same time, droplet size decreased considerably when the
250 maximum shear stress was stepped up from a low level (1 Pa) to a mid and high level (6 and 20 Pa),
251 where the droplet size was comparable. These findings were independent of emulsifier type. In the
252 case of the Tween 20 stabilised w/o/w emulsions (Figure 1A), the increase in emulsifier concentration
253 from 0.5% to 4% had little impact on the droplet size, as could be expected based on the much lower

254 literature value for this emulsifier's CMC reported in Table 2. On the other hand, the increase in Tween
255 20 concentration led to an improvement in the span for the intermediate maximum shear stress (6
256 Pa). This could be due to the presence of excess emulsifier molecules in the continuous emulsion
257 phase protecting the formed droplets against coalescence. In literature, 2% Tween 20 is often
258 reported for the production of uniform and stable w/o/w emulsions (Pawlik and Norton 2012,
259 Dragosavac et al., 2012 and Pradhan et al., 2014), and was therefore chosen as a constant in the
260 investigation of the other processing parameters on emulsion microstructure. For OSA starch
261 stabilised w/o/w emulsions (Figure 1B), the droplet size decreased when increasing OSA starch
262 concentration from 2% to 4%. This was accompanied with a span reduction to 0.53 for maximum
263 shear stress of 51 Pa. Further increase in starch concentration did not allow the formation of uniformly
264 sized w/o/w emulsions, potentially due to the associated large increase in external phase viscosity.
265 Therefore 4% OSA starch was used in further experiments. For PPI stabilised w/o/w emulsions (Figure
266 1C), a decrease in the droplet size was observed with increasing PPI concentration from 0.5% to 1.5%.
267 Once the PPI concentration was above 1.5%, no further decrease of the droplet size, while span
268 increased, was observed. Thus, 1.5% PPI was selected further on.

269 It is worth noting that the Tween 20 stabilised w/o/w emulsions had a smaller droplet size and slightly
270 better emulsion uniformity (lower span) compared to the OSA starch and PPI stabilised emulsions.
271 This can be explained by the higher surface activity of this low molecular weight emulsifier, as reported
272 in Table 2, and the faster adsorption rate at the interface compared to the complex emulsifiers starch
273 and protein (Bos and van Vliet, 2001, Kralova and Sjöblom, 2009). Nevertheless, values of span never
274 exceeded 1 when complex food emulsifiers were used.

275

276 3.2 Effect of maximum shear stress and injection rate

277 Both injection rate (1-15 ml min^{-1}) and maximum shear stress (1-51 Pa) have been proven in literature

278 to influence the mean droplet size and uniformity of w/o/w emulsions. Therefore, their joint influence
279 was studied experimentally within the Dispersion cell. Concentration of emulsifiers was optimised and
280 2% Tween 20, 4% OSA starch and 1.5% PPI was used to evaluate the maximum shear stress and
281 injection rate influence. Produced emulsions showed the characteristic appearance of a w/o/w
282 emulsion, namely dark appearance of the dispersed droplets. For illustration, one representative
283 image of one emulsion each stabilised with Tween 20, OSA starch and PPI at the lowest and the highest
284 maximum shear stress is shown in Figure 2.

285 Mean droplet size and span of the emulsions are presented in Figure 3 along with the model
286 predictions for droplet size (Equation 1). The experimental droplet sizes were larger than the predicted
287 data but followed the same decreasing trend with increasing maximum shear stress. As expected,
288 experimental data was closest to the model prediction at the lowest injection rate of 1 ml min^{-1}, and
289 findings agree with literature (Vladisavljevic and Schubert, 2003, Dragosavac et al., 2012, Holdich et
290 al., 2010).

291 When 2% Tween 20 was used as emulsifier, drops between 50 and 250 µm were produced with a span
292 below 0.7. At the low maximum shear stress (1 Pa), $d_{4,3}$ was larger than 200 µm, which is larger than
293 the spacing between the pores. This could mean that the newly formed emulsion droplets built up at
294 the membrane surface rather than immediately detached. Possibly, the small shear force applied with
295 the paddle led to the formation of a droplet layer on the membrane surface, which then slowly
296 dispersed into the bulk (Pawlik and Norton, 2012). Besides, it could be that not all of the membrane
297 pores were used to produce droplets during emulsification, providing more space for droplets to grow
298 on the membrane (Vladisavljevic and Schubert, 2002). When the lowest injection rate of 1 ml min^{-1}
299 was applied, uniform emulsion droplets with a span between 0.4 and 0.6 could be obtained. This also
300 suggests that not all membrane pores were active. If all membrane pores were active to produce
301 droplets, two neighbouring droplets would limit the droplet growth to interpore distance leading to a

lower span due to the additional push off force (Kosvintsev et al. 2005). The lowest span for the Tween 20 stabilised system was 0.49 and recorded for 1 ml min^{-1} injection rate and 10 Pa maximum shear stress. The highest span of approximately 0.65 was found when the highest injection rate of 15 ml min^{-1} and the extreme cases of the low (1 Pa) and high (20 Pa) end of the shear stress range was applied, which suggests fewer uniform droplets. This could be due to some large droplets being broken up by the paddle stirrer at the high maximum shear stress and droplets creaming at the low maximum shear stress or the highest injection rate (Dragosavac et al., 2012, Thompson et al., 2011).

When PPI was used to stabilise the w/o/w emulsions (Figure 3B) drops between 300 and 60 µm were produced with spans below 0.85. For the OSA starch as emulsifier (Figure 3C) drops between 350 and 65 µm were produced with spans below 1. The viscosity of the OSA starch solution was roughly 10x greater compared to the viscosity of the Tween and PPI solutions. Therefore, the greater span and larger droplet size of the emulsions stabilised with starch can be explained with the lower diffusivity of the molecules and longer time for drop stabilisation leading eventually to coalescence. As found for the Tween 20 stabilised system, when the lowest injection rate of 1 ml min^{-1} was applied, narrow droplet size distributions were generally produced with spans around 0.6 for the OSA starch and PPI stabilised systems. The lowest span for the OSA starch stabilised system was 0.4 when processed at 1ml min^{-1} injection rate and 5 Pa maximum shear stress. The lowest span for the PPI stabilised emulsions was 0.4 when processed at 10 ml min^{-1} injection rate and 1 Pa maximum shear stress.

The predicted droplet diameter decreased with increasing maximum shear stress for all emulsifiers (model line within Figure 3). As expected based on the interfacial tension values (see Table 2), the smallest droplet diameter was predicted for the Tween 20 (Figure 3A) stabilised emulsion, followed by PPI (Figure 3B) and then OSA starch (Figure 3C) stabilised systems, at all maximum shear stress values. The maximum shear stress range was extended to higher values for the OSA starch stabilised w/o/w emulsion due to its around tenfold higher viscosity of the continuous emulsion phase compared to the

326 other two systems (see Table 2). The maximum shear stress range of the predicted droplet diameter
327 curve for the Tween 20 and the PPI stabilised systems were very similar.

328 A relatively high maximum shear stress in the present set-up (14-51Pa) combined with a low injection
329 rate (i.e. 1 ml min^{-1}) yielded w/o/w emulsions for all three emulsifiers with comparable droplet size of
330 around 60-70 µm. As our intention for the Mg^{2+} encapsulation/release tests was to investigate the
331 influence of emulsifier independently of droplet size (to keep the surface area for the release constant)
332 droplets with a diameter of roughly 60 µm were produced according to the conditions from Figure 3.

333

334 3.3 Mid-term microstructure stability of the w/o/w emulsions

335 The coalescence stability of the w/o/w emulsions stabilised with 2% Tween 20, 4% OSA starch and 1.5%
336 PPI manufactured at 1ml min^{-1} injection rate and the three maximum shear stress levels (low, mid and
337 high) was investigated for up to 13 days after processing.

338 Figure 4 shows the corresponding droplet size distributions and micrographs. For each emulsion, the
339 droplet size distributions showed no difference over 13 days, which suggests these w/o/w emulsions
340 were stable against coalescence independent of emulsifier type and sample age. Although all w/o/w
341 emulsions creamed by visual observation, the micrographs show that there was no apparent change
342 in microstructure and no emptying out for any of the emulsions over the 13 day period of observation.
343 As it can be seen from Figure 4, even on day 13, the emulsion droplets had a dark appearance, which
344 demonstrates that there was little or no loss of the inner water droplets from the oil droplets of the
345 w/o/w emulsions.

346

347 3.4 Effect of continuous phase (w_2) on Mg^{2+} release and encapsulation

348 Magnesium release was tracked over a period of 13 days to explore encapsulation efficiency of
349 magnesium or the diffusion of the internal water phase (w_1) to the external water phase (w_2) of the
350 $w_1/o/w_2$ emulsions. These emulsions had xanthan gum added post emulsification to eliminate the
351 impact of creaming on the release data. According to section 3.2, similarly sized uniform droplets
352 (roughly 60 μm diameter), characterised by a low span, independent of emulsifier type were obtained
353 when a low injection rate (1 ml min^{-1}) was combined with the maximum shear stress of 14, 16 and 36
354 Pa for Tween 20, PPI and OSA starch (see Figure 3). For production of w/o/w emulsions for the release
355 measurement sodium chloride was substituted for magnesium as a more convenient marker molecule
356 (see section 2.6). To maximise the observation window, the volume fraction of w_1/o in w/o/w
357 emulsions was increased from 10 vol.% to 30 vol.%. So, initially it was ascertained through microscopic
358 inspection and acquisition of droplet size distribution data that these two formulation changes had no
359 impact on the microstructure of the w/o/w emulsions. There was no apparent change in the
360 microstructure of the w/o/w emulsions when using Mg^{2+} instead of NaCI in w_1 compared to the
361 respective microstructure shown in Figure 3 on the day of emulsion processing and on day 13
362 (micrographs omitted for sake of brevity).

363 Figure 5 shows the release of magnesium from w_1 into w_2 of the xanthan gum thickened w/o/w
364 emulsions over 13 days. It has been widely reported that an increase in the viscosity of aqueous phases
365 in w/o/w emulsions by the addition of thickening and gelling agents leads to an improvement in the
366 encapsulation efficiency of w/o/w emulsions (Kim et al., 2017, Oppermann et al., 2018). Although
367 viscosity change induced by xanthan gum was expected to play a significant role on the encapsulation
368 efficiency, there were differences found in the released amount of magnesium from all xanthan gum
369 added w/o/w emulsions depending on emulsifier type. Encapsulation efficiency immediately after
370 production was 100% for the OSA starch and PPI stabilised w/o/w emulsions. The OSA starch and PPI
371 stabilised w/o/w emulsions showed some release only between day 3 and day 6 after emulsion
372 preparation. Approximately 1% of magnesium were detected in w_2 on day 6. Release continued at a

373 slow rate and reached roughly 3% on day 13. So, these two types of emulsions appeared relatively
374 stable against magnesium release from the encapsulated water phase, thus it is assumed that there
375 was limited diffusion of w_1 into w_2 setting on only between 3 and 6 days after emulsion generation.

376 The Tween 20 stabilised w/o/w emulsion was less stable against magnesium release. 5% magnesium
377 release was noted on the day of emulsion processing meaning that encapsulation efficiency of 2%
378 Tween was 95%. This could be indicative of a rapid setting on of diffusion of w_1 into w_2, or loss of w_1
379 into w_2 during the emulsification process. Magnesium continuously leaked into the external water
380 phase albeit at decreasing rate over time. Similar observations for Tween 20 stabilised w/o/w
381 emulsions, but manufactured at a higher injection speed (about 5 ml min^{-1}), so having a larger droplet
382 size ($d_{3,2}$ = 107 µm), and encapsulating copper in w_1, have previously been reported (Dragosavac et al.,
383 2012). In that case around 50% of the encapsulated copper was released and w/o/w drops appeared
384 clear within 13 days of emulsion generation. In the current study, there was no apparent change in the
385 droplet appearance of Tween 20 stabilised w/o/w emulsions after 13-day storage. However, a loss of
386 27% of internal water phase (w_1) into w_2 by day 13 has been detected. Nevertheless, this loss might
387 not be enough to visibly change the appearance of the droplets, but diffusion of w_1 into w_2 might still
388 have occurred. Water and water soluble material transport in w/o/w emulsions can be explained either
389 by a swelling-breakdown mechanism or diffusion and/ or permeation through the oil film (Cheng et
390 al., 2007). Specifically, mechanisms behind diffusion and/ or permeation including an osmotic pressure
391 gradient between two aqueous phases (Matsumoto et al., 1980), the thin lamellae of surfactant which
392 partially form in the oil layer due to fluctuations in its thickness (Jager-Lezer et al., 1997, Garti, 1997b),
393 or reverse micelles in the oil phase (Sela et al., 1995) have previously been reported. Since the osmotic
394 pressure was balanced in this study, water transport between two aqueous phases and release of
395 magnesium might result from the thin lamellae of surfactant forming in the oil film and the PGPR
396 micelles and/or Tween 20 reverse micelles in the oil phase.

4 Conclusions

This research has for the first time shown that complex food emulsifiers such as starch and protein can be applied to produce stable w/o/w emulsions with the technology of stirred cell membrane emulsification. One should consider though that stabilisation with a low molecular surfactant such as Tween 20 would allow formation of slightly more uniform droplet size distributions (lower span) with a lower mean diameter. For the release of magnesium from the internal water phase to the external water phase, OSA starch and PPI stabilised w/o/w emulsions thickened by xanthan gum showed a better stability against release than Tween 20 stabilised ones. The results reported in this study enabled the production of uniformly sized w/o/w emulsions with similar average droplet diameters and high encapsulation efficiency using complex food emulsifiers. Immediately after production encapsulation efficiency for OSA starch and PPI was 100% while for Tween it was 97%. Delayed release was obtained when complex food emulsifiers (starch and protein) were used with almost no release up to 2 days. After 13 days, the emulsions stabilised with Tween 20 had released almost 30% of Mg^{2+} and for those stabilised with starch and protein Mg^{2+} leakage was less than 4%. This study has introduced a pathway, beneficial for food and pharmaceutical applications, to enhance the stability and encapsulation efficiency of w/o/w emulsions based on the appropriate selection of the hydrophilic emulsifier. Low energy membrane emulsification process proved to be a worthy tool to control as desired, both the droplet size of w/o/w emulsions independent of the hydrophilic emulsifier. Future work will focus on incorporation of volatile flavours within the emulsion matrix stabilised by complex food emulsifiers (PPI and starch).

Acknowledgement

XP acknowledges the scholarship from China Scholarship Council (CSC).

References

BAHTZ, J., GUNES, D. Z., SYRBE, A., MOSCA, N., FISCHER, P. & WINDHAB, E. J. (2016). Quantification of spontaneous w/o emulsification and its impact on the swelling kinetics of multiple w/o/w emulsions. *Langmuir,* 32**,** 5787-5795.

BHOSALE, R. & SINGHAL, R. 2006. Process optimization for the synthesis of octenyl succinyl derivative of waxy corn and amaranth starches. *Carbohydrate Polymers,* 66**,** 521-527.

BONNET, M., CANSELL, M., BERKAOUI, A., ROPERS, M. H., ANTON, M. & LEAL-CALDERON, F. 2009. Release rate profiles of magnesium from multiple W/O/W emulsions. *Food Hydrocolloids,* 23**,** 92-101.

BOS, M., A. & VAN VLIET, T. 2001. Interfacial rheological properties of adsorbed protein layers and surfactants: a review. *Advances in Colloid and Interface Science,* 91**,** 437-471.

CHEN, X., MCCLEMENTS, D. J., WANG, J., ZOU, L., DENG, S., LIU, W., YAN, C., ZHU, Y., CHENG, C. & LIU, C. 2018. Coencapsulation of (−)-Epigallocatechin-3-gallate and Quercetin in Particle-Stabilized W/O/W Emulsion Gels: Controlled Release and Bioaccessibility. *Journal of Agricultural and Food Chemistry*.

CHENG, J., CHEN, J.-F., ZHAO, M., LUO, Q., WEN, L.-X. & PAPADOPOULOS, K. D. 2007. Transport of ions through the oil phase of W-1/O/W-2 double emulsions. *Journal of Colloid and Interface Science,* 305**,** 175-182.

COTTRELL, T. & VAN PEIJ, J. (2015). Sorbitan esters and polysorbates. *In:* NORN, V. (ed.) *Emulsifiers in food technology.* West Sussex, UK: Wiley Blackwell.

DICKINSON, E. 2010. Flocculation of protein-stabilized oil-in-water emulsions. *Colloids Surf B Biointerfaces,* 81**,** 130-40.

DRAGOSAVAC, M. M., HOLDICH, R. G., VLADISAVLJEVIĆ, G. T. & SOVILJ, M. N. 2012. Stirred cell membrane emulsification for multiple emulsions containing unrefined pumpkin seed oil with uniform droplet size. *Journal of Membrane Science,* 392–393**,** 122-129.

DRAGOSAVAC, M. M., SOVILJ, M. N., KOSVINTSEV, S. R., HOLDICH, R. G. & VLADISAVLJEVIĆ, G. T. 2008. Controlled production of oil-in-water emulsions containing unrefined pumpkin seed oil using stirred cell membrane emulsification. *Journal of Membrane Science,* 322**,** 178-188.

GARTI, N. 1997b. Progress in stabilization and transport phenomana of double emulsions in food applications. *Lebensm.-Wiss.u.-Technol,* 30**,** 222-235.

GHARSALLAOUI, A., CASES, E., CHAMBIN, O. & SAUREL, R. (2009). Interfacial and emulsifying characteristics of acid-treated pea protein. *Food Biophysics,* 4**,** 273-280.

HERZI, S. & ESSAFI, W. 2018. Different magnesium release profiles from W/O/W emulsions based on crystallized oils. *Journal of Colloid and Interface Science,* 509**,** 178-188.

HOLDICH, R. G., DRAGOSAVAC, M. M., VLADISAVLJEVIĆ, G. T. & KOSVINTSEV, S. R. 2010. Membrane emulsification with oscillating and stationary membranes. *Industrial & Engineering Chemistry Research,* 49**,** 3810-3817.

ILIĆ, J. D., NIKOLOVSKI, B. G., PETROVIĆ, L. B., KOJIĆ, P. S., LONČAREVIĆ, I. S. & PETROVIĆ, J. S. 2017. The garlic (A. sativum L.) extracts food grade W1/O/W2 emulsions prepared by homogenization and stirred cell membrane emulsification. *Journal of Food Engineering,* 205**,** 1-11.

463 JAGER-LEZER, N., TERRISSE, I., BRUNEAU, F., TOKGOZ, S., FERREIRA, L., CLAUSSE, D., SEILLER, M. &
464 GROSSIORD, J. L. 1997. Influence of lipophilic surfactant on the release kinetics of water-
465 soluble molecules entrapped in a W/O/W multiple emulsion. *Journal of Controlled Release,*
466 45**,** 1-13.
467 JOSCELYNE, S. M. & TRAGARDH, G. 2000. Membrane emulsification - a literature review. *Journal of*
468 *Membrane Science,* 169**,** 107-117.
469 KASPRZAK, M. M., MACNAUGHTAN, W., HARDING, S., WILDE, P. & WOLF, B. 2018. Stabilisation of oil-
470 in-water emulsions with non-chemical modified gelatinised starch. *Food Hydrocolloids,* 81**,**
471 409-418.KIM, Y.-L., MUN, S., RHO, S.-J., DO, H. V. & KIM, Y.-R. 2017. "Influence of
472 physicochemical properties of enzymatically modified starch gel on the encapsulation
473 efficiency of W/O/W emulsion containing NaCl". *Food and Bioprocess Technology,* 10**,** 77-88.
474 KOSVINTSEV, S. R., GASPARINI, G., HOLDICH, R. G., CUMMING, I. W. & STILLWELL, M. T. 2005.
475 Liquid–liquid membrane dispersion in a stirred cell with and without controlled shear.
476 *Industrial & Engineering Chemistry Research,* 44**,** 9323-9330.
477 KRALOVA, I. & SJÖBLOM, J. 2009. Surfactants used in food industry: a review. *Journal of Dispersion*
478 *Science and Technology,* 30**,** 1363-1383.
479 KRSTONOŠIĆ, V., DOKIĆ, L. & MILANOVIĆ, J. (2011). Micellar properties of OSA starch and interaction
480 with xanthan gum in aqueous solution. *Food Hydrocolloids,* 25**,** 361-367.
481 LEADI COLE, M. & L. WHATELEY, T. 1997. Release rate profiles of theophylline and insulin from stable
482 multiple w/o/w emulsions. *Journal of Controlled Release,* 49**,** 51-58.
483 MANICKAM, S., MUTHOOSAMY, K. & RAVIADARAN, R. 2018. Simple and Multiple Emulsions
484 Emphasizing on Industrial Applications and Stability Assessment. *Food Process Engineering*
485 *and Quality Assurance.* Apple Academic Press.
486 MATSUMOTO, S., INOUE, T., KOHDA, M. & IKURA, K. 1980. Water permeability of oil layers in W/O/W
487 emulsions under osmotic pressure gradients. *Journal of Colloid and Interface Science,* 77**,** 555-
488 563.
489 NIKOLOVSKI, B. G., BAJAC, J. D., MARTINOVIC, F. L. & BOGUNOVIĆ, N. 2018. Optimizing stirred cell
490 membrane emulsification process for making a food-grade multiple emulsion. *Chemical*
491 *Papers,* 72**,** 533-542.
492 O' KANE, F. E., VEREIJKEN, J. M., GRUPPEN, H. & VAN BOEKEL, M. 2005. Gelation behavior of protein
493 isolates extraded from 5 cultivars of Pisum sativum L. *Journal of Food Science,* 70**,** C132-C137.
494 OBRADOVIĆ, S. & POŠA, M. (2017). The influence of the structure of selected Brij and Tween
495 homologues on the thermodynamic stability of their binary mixed micelles. *The Journal of*
496 *Chemical Thermodynamics,* 110**,** 41-50.
497 OPPERMANN, A. K. L., NOPPERS, J. M. E., STIEGER, M. & SCHOLTEN, E. 2018. Effect of outer water
498 phase composition on oil droplet size and yield of (w1/o/w2) double emulsions. *Food Research*
499 *International,* 107**,** 148-157.
500 PAWLIK, A., COX, P. W. & NORTON, I. T. 2010. Food grade duplex emulsions designed and stabilised
501 with different osmotic pressures. *J Colloid Interface Sci,* 352**,** 59-67.
502 PAWLIK, A. K. & NORTON, I. T. 2012. Encapsulation stability of duplex emulsions prepared with SPG
503 cross-flow membrane, SPG rotating membrane and rotor-stator techniques-A comparison.
504 *Journal of Membrane Science,* 415**,** 459-468.
505 PRADHAN, R., KIM, Y.-I., JEONG, J.-H., CHOI, H.-G., YONG, C. S. & KIM, J. O. 2014. Fabrication,
506 Characterization and Pharmacokinetic Evaluation of Doxorubicin-Loaded Water-in-Oil-in-
507 Water Microemulsions Using a Membrane Emulsification Technique. *Chemical and*
508 *Pharmaceutical Bulletin,* 62**,** 875-882.
509 SCHRÖDER, V., BEHREND, O. & SCHUBERT, H. 1998. Effect of Dynamic Interfacial Tension on the
510 Emulsification Process Using Microporous, Ceramic Membranes. *Journal of Colloid and*
511 *Interface Science,* 202**,** 334-340.

SCHUBERT, H. & AX, K. 2003. Engineering food emulsions. *In:* MCKENNA, B. M. (ed.) *Texture in food, volume 1: semid-solid foods.* 1st Edition ed. Boca Raton, FL, USA: CRC Press.

SCHUBERT, H., AX, K. & BEHREND, O. 2003. Product engineering of dispersed systems. *Trends in Food Science & Technology,* 14**,** 9-16.

SCHUCH, A., DEITERS, P., HENNE, J., KOHLER, K. & SCHUCHMANN, H. P. 2013. Production of W/O/W (water-in-oil-in-water) multiple emulsions: droplet breakup and release of water. *Journal of Colloid and Interface Science,* 402**,** 157-64.

SCHUCH, A., WRENGER, J. & SCHUCHMANN, H. P. 2014. Production of W/O/W double emulsions. Part II: Influence of emulsification device on release of water by coalescence. *Colloids and Surfaces A: Physicochemical and Engineering Aspects,* 461**,** 344-351.

SELA, Y., MAGDASSI, S. & GARTI, N. 1995. Release of markers from the inner water phase of W/O/W emulsions stabilized by silicone based polymeric surfactants. *Journal of controlled release,* 33**,** 1-12.

SHOGREN, R. L., VISWANATHAN, A., FELKER, F. & GROSS, R. A. (2000). Distribution of octenyl succinate groups in octenyl succinic anhydride modified waxy maize starch. *Starch - Stärke,* 52**,** 196-204.

SILVA, W., TORRES-GATICA, M. F., OYARZUN-AMPUERO, F., SILVA-WEISS, A., ROBERT, P., COFRADES, S. & GIMÉNEZ, B. 2018. Double emulsions as potential fat replacers with gallic acid and quercetin nanoemulsions in the aqueous phases. *Food Chemistry,* 253**,** 71-78.

SPYROPOULOS, F., LLOYD, D. M., HANCOCKS, R. D. & PAWLIK, A. K. 2014. Advances in membrane emulsification. Part A: recent developments in processing aspects and microstructural design approaches. *Journal of the Science of Food and Agriculture,* 94**,** 613-627.

STAUFFER, C. E. 1999. *Emulsifiers,* St. Paul, Minnesota, Eagan Press.

THOMPSON, K. L., ARMES, S. P. & YORK, D. W. 2011. Preparation of Pickering Emulsions and Colloidosomes with Relatively Narrow Size Distributions by Stirred Cell Membrane Emulsification. *Langmuir,* 27**,** 2357-2363.

USHIKUBO, F. Y. & CUNHA, R. L. (2014). Stability mechanisms of liquid water-in-oil emulsions. *Food Hydrocolloids,* 34**,** 145-153.

VAN DER GRAAF, S., SCHROËN, C. G. P. H. & BOOM, R. M. 2005. Preparation of double emulsions by membrane emulsification—a review. *Journal of Membrane Science,* 251**,** 7-15.

VLADISAVLJEVIC, G. T. & SCHUBERT, H. 2002. Preparation and analysis of oil-in-water emulsions with a narrow droplet size distribution using Shirasu-porous-glass (SPG) membranes. *Desalination,* 144**,** 167-172.

VLADISAVLJEVIC, G. T. & SCHUBERT, H. 2003. Influence of process parameters on droplet size distribution in SPG membrane emulsification and stability of prepared emulsion droplets. *Journal of Membrane Science,* 225**,** 15-23.

WALSTRA, P. 1993. Principles of emulsion formation. *Chemical Engineering Science,* 48**,** 333-349.

WALSTRA, P. & SMULDERS, P. E. A. 1998. Emulsion formation. *In:* BINKS, B. P. (ed.) *Modern aspects of emulsion science.* 1st Edition ed. Cambridge, UK: The Royal Society of Chemistry.

552 List of tables
553
554 Table 1: Averaged interfacial tension, viscosity (at 10 s^{-1}) and density data acquired at 20 °C.
555

556 Table 2: Physicochemical properties of emulsifiers used in this study. CMC: critical micelle
557 concentration.

558
559
560

561 Table 1: Averaged interfacial tension, viscosity (at 10 s^{-1}) and density data acquired at 20 °C

w_2	interfacial tension at w_1/o interface (mN/m)	viscosity (mPa.s)	density (g/cm^3)
2% Tween 20 in 0.1 M NaCl	5.9 ± 0.4	1.07 ±0.01	1.0050 ± 0.0000
4% OSA starch in 0.1 M NaCl	13.7 ± 0.2	11.57 ± 0.12	1.0173 ± 0.0000
1.5% PPI in 0.1 M NaCl	10.5 ± 0.4	1.26 ± 0.05	1.0065 ± 0.0002

562

563

564

565 Table 2: Physicochemical properties of emulsifiers used in this study. CMC: critical micelle
566 concentration .

Emulsifier	Approximate molecular weight (g/mol)	Approximate CMC	Structural formula
PGPR	3000 (Ushikubo and Cunha, 2014)	1.8 (% w/w) at 20 °C (Bahtz et al., 2016)	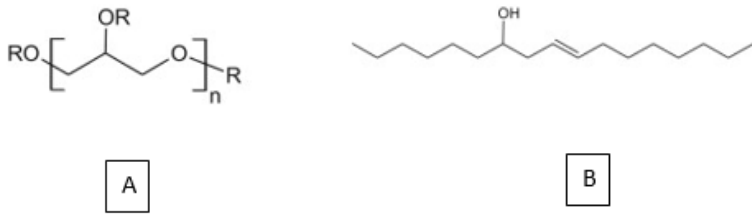 A) chemical structure of PGPR. R is a hydrogen, ricinoleic acid or polyricinoleic acid. The average value of n is about 3. B) chemical structure of ricinoleic acid. (Ushikubo and Cunha, 2014)
Tween 20	1228 (Obradović and Poša, 2017)	0.07 (% w/w) at 25°C (Cottrell and Van Peij, 2015)	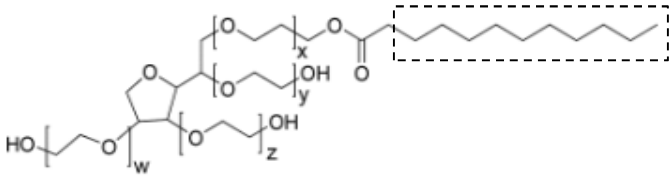 Dotted box notes the alkyl chain. (Obradović and Poša, 2017)
OSA starch	470000 (Kasprzak et al., 2018)	0.05 (% w/v) at 25°C (Krstonošić et al., 2011)	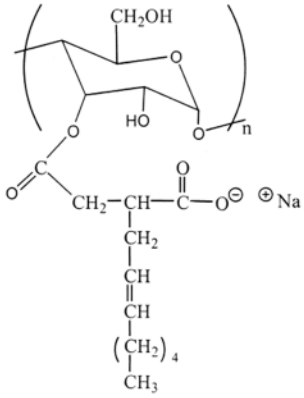 (Shogren et al., 2000)
PPI	Main components (O' Kane et al., 2005): legumin, 380000 g/mol; vicilin, 150000 g/mol.	0.04 (% w/w) at 20 °C (Gharsallaoui et al., 2009)	-

567

568

569

Appendix:

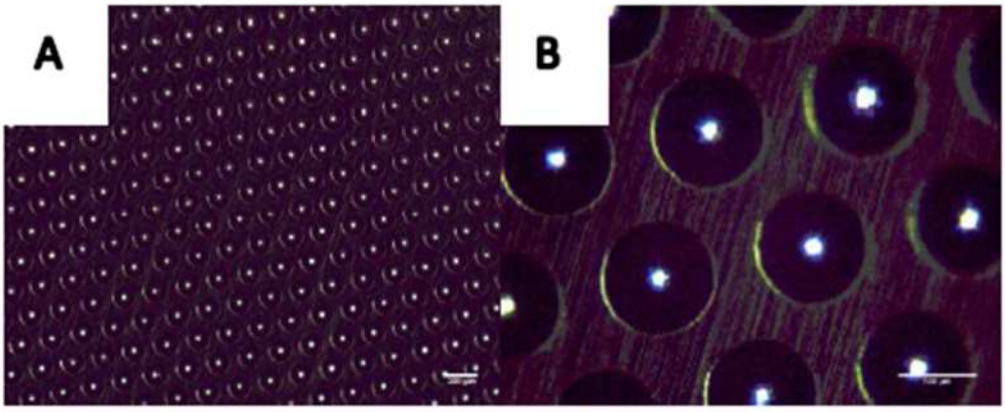

Figure A1: Micrographs of the membrane with a pore diameter of 20 µm and a pore spacing of 200 µm. The scale bar in A and B represents 200 µm and 100 µm respectively.

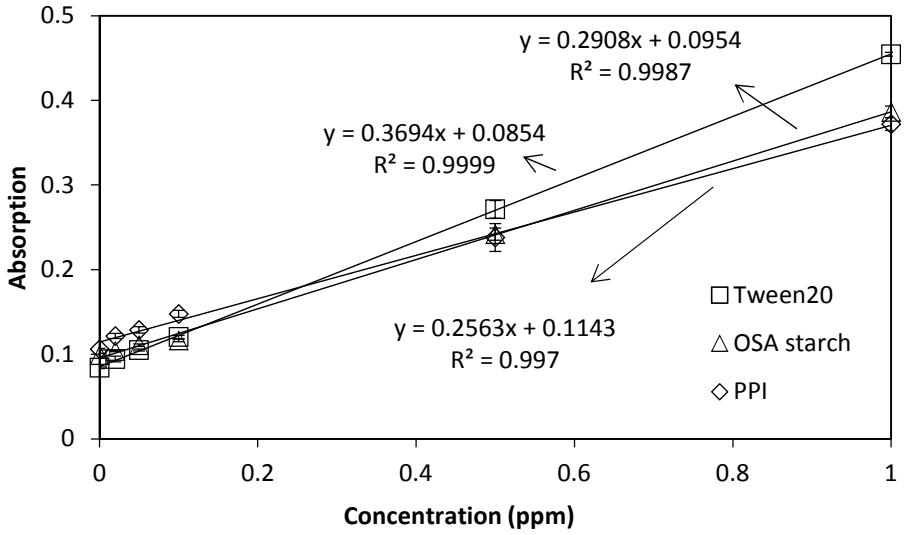

Figure A2: Standard curves of magnesium in standard solutions with Tween20, OSA starch or PPI.